

“Defective” Logic: Using spatiotemporal patterns in coupled relaxation oscillator arrays for computation

Shakti N. Menon and Sitabhra Sinha
The Institute of Mathematical Sciences,
CIT Campus, Taramani, Chennai 600113, India
Email: shakti@imsc.res.in, sitabhra@imsc.res.in

Abstract—An intriguing interpretation of the time-evolution of dynamical systems is to view it as a computation that transforms an initial state to a final one. This paradigm has been explored in discrete systems such as cellular automata models, where the relation between dynamics and computation has been examined in detail. Here, motivated by microfluidic experiments on arrays of chemical oscillators, we show that computation can be achieved in continuous-state, continuous-time systems by using complex spatiotemporal patterns generated through a reaction-diffusion mechanism in coupled relaxation oscillators. We present two paradigms that illustrate this computational capability, namely, using perturbations to (i) generate propagating configurations in a system of initially exactly synchronized oscillators, and (ii) transform one time-invariant pattern to another. In particular, we have demonstrated a possible implementation of NAND logic. This raises the possibility of universal computation in such systems as all logic gates can be constructed from NAND gates. Our work suggests that more complex schemes can potentially implement arbitrarily complicated computation using reaction-diffusion processes, bridging pattern formation with universal computability.

I. INTRODUCTION

The physical world abounds with dynamical systems in which the temporal evolution of states results in processes as complex as life. The usual approach for understanding the mechanisms underlying such phenomena is to model them as a system of differential (or difference) equations and to analyze the resulting spatiotemporal patterns. An alternative viewpoint is to consider these processes as computations that transform input states into output states iteratively. This suggests an intimate relation between the physical world and that of information, an idea which has led to suggestions that the universe itself may be viewed as a computer [1]. Indeed, the mutual connection between ‘it’ and ‘bit’ [2] has been proposed in light of the fact that computational simulations may help provide insights into the nature of physical laws [3] while, in turn, physical principles provide constraints on the kind of computations that are feasible [4]. These insights have inspired several studies on the connection between spatiotemporal patterns generated by dynamical systems and the computational processes that they might represent [5], e.g., in models of neuronal networks [6]. In this context, cellular automata is the most commonly studied class of dynamical models [7], as their states, which form a countably finite set, evolve in discrete space and time thus allowing for an intuitive connection with existing abstract models of computation, such as the Turing

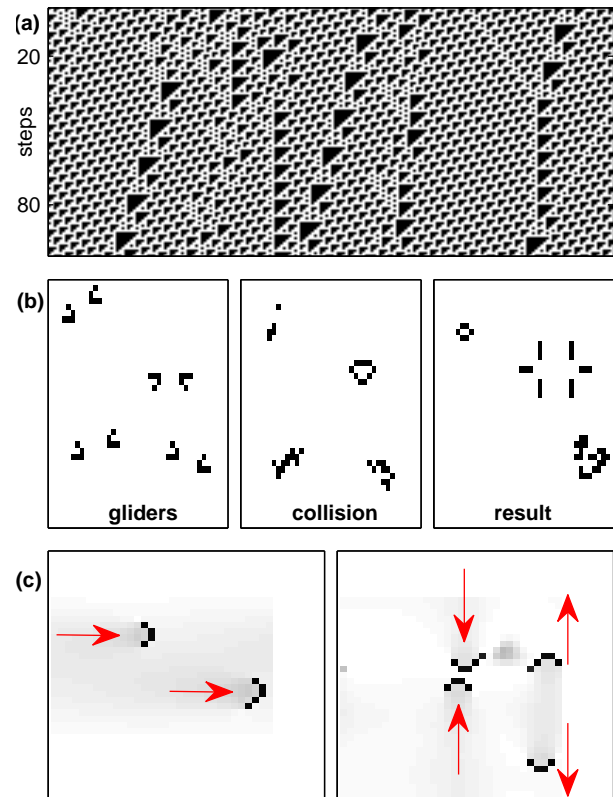


Fig. 1. (a) Spatiotemporal patterns in the dynamical evolution of *Rule 110*, a one-dimensional cellular automaton that has been shown to be capable of universal computation [11]. (b) Snapshots of the temporal evolution of Conway’s “*Game of Life*”, a two-dimensional cellular automaton, showing (from left to right) different stages of the collisions between propagating coherent structures known as “gliders”. The use of gliders and more complex structures in the construction of different types of logic gates has given weight to the claim that this cellular automaton is capable of universal computation [12]. (c) Propagating structures corresponding to phase defects in a two-dimensional lattice of diffusively coupled relaxation oscillators [13]. The left panel shows two coherent structures, resembling the gliders of (b), moving horizontally in the direction indicated by the arrows, while the right panel shows the interaction (via collision) between pairs of vertically moving glider-like structures.

Machine [8].

While different types of cellular automata had been investigated and classified based on the nature of the patterns

manifested through their spatiotemporal dynamics [9], it has recently been shown that they can also be classified in terms of their computational complexity [10]. Certain classes of cellular automata have been shown to be capable of universal computation [11], a property which has been connected with the existence of propagating coherent structures, such as “gliders” [12] in the two-dimensional cellular automata *Conway’s Game of Life* [Fig. 1(a-b)]. Similar structures have recently been observed in spatially extended arrays of diffusively coupled relaxation oscillators that model certain chemical systems [13]. These structures, such as the propagating phase discontinuities (‘defects’) in the array shown in Fig. 1 (c) are visually analogous to the gliders in cellular automata. This brings up the intriguing possibility of using interactions between these defects, and other spatiotemporal pattern regimes observed in this system for computation. Indeed, the potential of computing through chemical systems has been explored earlier, e.g., in the contexts of enzyme-substrate reactions [14], waves in excitable membranes [15] and bubbles in microfluidic devices [16]. However, the system we explore differs from the earlier proposals in that oscillations (viz., in the concentrations of the active species) play a fundamental role in enabling computation. As interactions between biochemical oscillators through reaction-diffusion mechanism [17] is thought to be a critical component for living systems [18], the demonstration of computing via chemical oscillations presents a direct connection between information processing and the process of life.

In this article we introduce two paradigms for implementing computation using local perturbations on the collective dynamics of a model system of coupled relaxation oscillators. As the model system under consideration has close connections to the experimental setup for microfluidic chemical oscillators, this suggests that the principles we have presented here can be used for constructing chemical logic gates [19]. Note that an important distinction between oscillator arrays and cellular automata lies in the fact that the former are usually described by systems of coupled differential equations, and therefore have a continuous state space in which the system evolves in continuous time. Thus, computations implemented in terms of chemical oscillations will be defined over a space of real numbers [20] rather than a countably finite number of states as in cellular automata. Furthermore, although glider-like configurations can be shown in two-dimensional realizations of our model system, here we focus on one-dimensional arrays for ease of understanding. The demonstration of the capacity for computing even in such simple systems underscores the potential inherent in higher-dimensional realizations.

II. MODEL

The spatiotemporal dynamics of an oscillatory chemical system is investigated here by using a one-dimensional ring of N relaxation oscillators, each diffusively coupled to its two nearest neighbors. The local dynamics of individual oscillators are all identical, being described by the generic FitzHugh-Nagumo (FHN) model which is a phenomenological representation of the mechanism underlying periodic activity in many chemical and biological systems [21]. This model comprises a pair of dynamical variables u and v that correspond to a fast activation and a slow inactivation process, respectively,

described by

$$\begin{aligned} \dot{u} &= f(u, v) = u(1-u)(u-\alpha) - v, \\ \dot{v} &= g(u, v) = \epsilon(ku - v - b), \end{aligned} \quad (1)$$

where $\alpha = 0.139$, $k = 0.6$ are parameters describing the kinetics, $\epsilon = 0.001$ characterizes the recovery rate and b is a measure of the asymmetry of the oscillator (measured as the ratio of the time spent by the oscillator at high and low value branches of u). The parameter values are chosen such that the system is in the oscillatory regime, and we have verified that small variations in these values do not affect our results qualitatively. The state of each oscillator at any given time is characterized by its normalized phase angle $\phi \in [0, 1]$ that measures the position of the oscillator on its limit cycle relative to the location of the peak of the activation variable (considered to be the origin, i.e., $\phi = 0$).

In chemical experiments involving oscillatory media, beads containing the reactive solution are suspended in a chemically inert medium that allows passage of only the inhibitory chemical species [22]. Analogous to this, the oscillators in our model are diffusively coupled via the inactivation variable v . The dynamics of the resulting system is described by

$$\begin{aligned} \dot{u}_i &= f(u_i, v_i), \\ \dot{v}_i &= g(u_i, v_i) + D_v(v_{i-1} + v_{i+1} - 2v_i), \end{aligned} \quad (2)$$

where $i = 1, 2, \dots, N$, and the ring connection topology is implemented through the use of periodic boundary conditions ($v_0 = v_N$ and $v_{N+1} = v_1$). The diffusion constant D_v represents the strength of coupling between neighboring relaxation oscillators that are connected through their inactivation variables. The dynamical equations are solved using an adaptive Runge-Kutta scheme. To identify the dynamical regimes in the $b - D_v$ parameter space, the system behavior is analyzed over many (10^3) realizations, with each oscillator having a random initial phase, chosen from a uniform distribution.

III. RESULTS

The system shows a range of spatiotemporal patterns including (a) Exact Synchronization (ES) of all elements in the ring, i.e., all oscillators have the same phase, (b) Anti-Phase Synchronization (APS) where oscillators next to each other are in opposite phase, (c) Spatially Patterned Oscillator Death (SPOD) where the oscillators are arrested in different stationary states, and (d) Chimera States (CS), where oscillating elements coexist with elements having nearly stationary behavior. In addition to these, several other possible types of spatiotemporal patterns may be observed, and are categorized under a Miscellaneous (Misc) class [13]. This includes several types of propagating phase defects [Fig. 2(a)]. Both APS and SPOD states have been reported earlier in experiments on chemical systems [22] and it is likely that the other dynamical patterns seen in our simulations can also be reproduced in appropriately designed experiments.

The robustness of these patterns are related to the size of their basins of attraction (i.e., the fraction of randomly chosen initial conditions that lead to a specific pattern) in the $(b - D_v)$ parameter space [Fig. 2(b)]. Distinct pattern regimes were identified using several order parameters that are described in detail in Ref. [13]. Regions in parameter space where ES, APS,

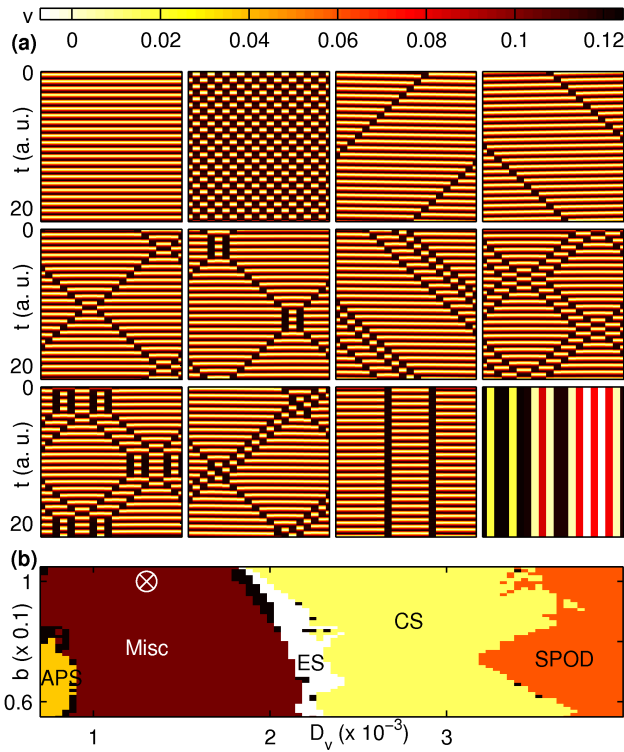


Fig. 2. (a) Spatiotemporal evolution of a ring of $N = 20$ relaxation oscillators, each coupled diffusively to their nearest neighbors through the inactivation variable. The individual oscillators are identical and described by the FitzHugh-Nagumo equations (see text) with parameters $\epsilon = 0.001$, $k = 0.6$, $b = 0.1$ and $\alpha = 0.139$. The strength of the diffusive coupling is $D_v = 1.13 \times 10^{-3}$ for all panels except for the bottom right, in which $D_v = 4 \times 10^{-3}$ was used. The displayed patterns, obtained using different initial states, are (left to right, top to bottom): Exact Synchronization (ES), Anti-Phase Synchronization (APS), a Left-moving defect (L), a Right-moving defect (R), a pair of Left and Right moving defects (LR) that collide and pass through, a pair of Left and Right moving defects whose collision results in a brief period of interaction before they pass through (LR (long)), three defects moving in the same direction (3L/3R), two left and two right moving defects (2LR) that collide and pass through, two left and two right moving defects whose collisions result in a brief period of interaction before they pass through (2LR (long)), moving defects other than those described above (Others), two Static defects (2S) where a pair of oscillators remain arrested in a stationary state, and a Spatially Patterned Oscillator Death (SPOD) state. In each panel, time is expressed in arbitrary units, normalized with respect to the period of the individual oscillators. (b) Different dynamical regimes observed in a ring of $N = 20$ oscillators in the $(D_v - b)$ parameter plane, showing regions where the majority ($> 50\%$) of initial states result in ES, APS, SPOD, Chimera State (CS) and Miscellaneous patterns (Misc). Regions colored black indicate parameter regimes where no single class of patterns were observed for a majority of initial states. The circled cross marks the location in parameter space where the dynamical patterns (except SPOD) shown in the panels of (a) are obtained. The parameter values for the individual oscillators are $\epsilon = 0.001$, $k = 0.6$ and $\alpha = 0.139$.

SPOD, CS and Misc states are observed for the majority of initial conditions (i.e., $> 50\%$ of the realizations) are labeled correspondingly in Fig. 2(b). Over a small region of parameter space in the Misc regime of Fig. 2(b), we observe patterns characterized by one or more discontinuities of phase along the oscillator ring (referred to as phase defects) that move against a background of synchronized oscillations. The initial interactions between two defects moving in opposite directions result either in their reflection or in the annihilation of one or both of them. In the steady state, one finds that a conserved

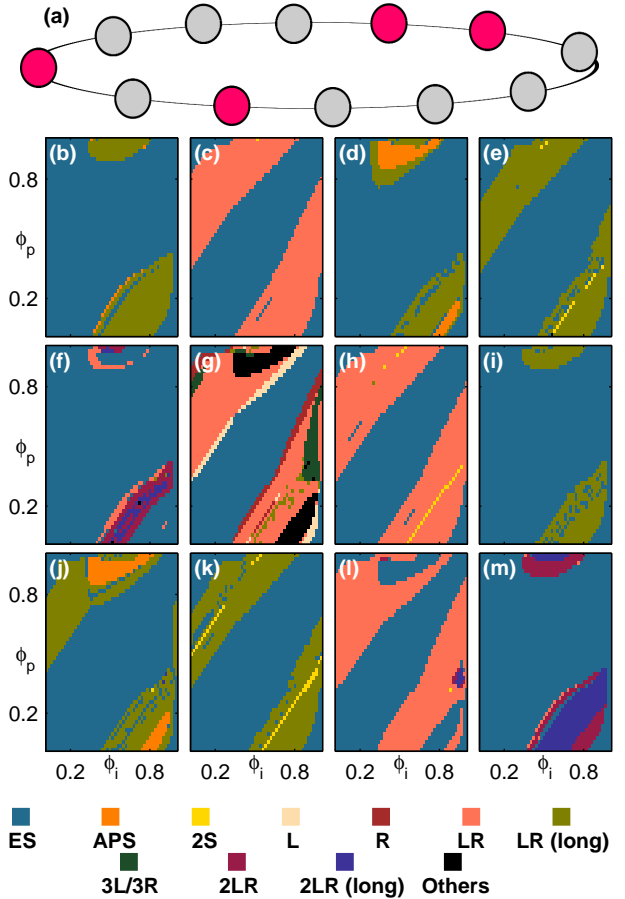


Fig. 3. (a) Schematic diagram illustrating the principle used to generate different types of defects through local perturbations to an initial ES state. Each circle represents an oscillator that is coupled diffusively to its nearest neighbor (via the inactivation variable). When the synchronized oscillators are at some phase ϕ_i on the limit cycle, local perturbations are applied to certain oscillators (shown in pink) by changing their phase to ϕ_p , also on the limit cycle. The perturbation scheme illustrated in this schematic can have numerous representations because of the circular symmetry. One such representation is 10100011... (taking the bottom-most perturbed oscillator as the origin and moving clockwise), where 0 and 1 correspond to unperturbed and perturbed oscillators, respectively. (b-m) Perturbation response ($\phi_i - \phi_p$) diagrams indicating the nature of the defect patterns (represented using the color scheme shown below the panels) obtained when a system of $N = 20$ oscillators in an initial ES state is perturbed according to the principle outlined in (a). Each oscillator is identical, being described by the parameter values $\epsilon = 0.001$, $k = 0.6$, $b = 0.1$ and $\alpha = 0.139$, and is coupled diffusively to each neighbour with strength $D_v = 1.13 \times 10^{-3}$. The perturbation schemes used to generate the response diagrams shown in the panels are: (b) 1000..., (c) 1100..., (d) 1010..., (e) 1110..., (f) 1001..., (g) 1011..., (h) 1111..., (i) 10001..., (j) 10101..., (k) 11111..., (l) 101101..., and (m) $10^8 1$..., where $10^k 1$ indicates that there are k unperturbed oscillators between two perturbed ones.

number of defects can reflect off each other indefinitely.

The resemblance of these propagating defects to the coherent structures in cellular automata mentioned earlier suggests that the former may be used to implement a form of computation. A possible approach is to perturb a system that is in an ES state with a signal that acts as the input for a computation. Specifically, this involves resetting the initial phase (ϕ_i) of selected oscillators in the ring to another phase (ϕ_p). The sites that are perturbed are indicated by 1, while the

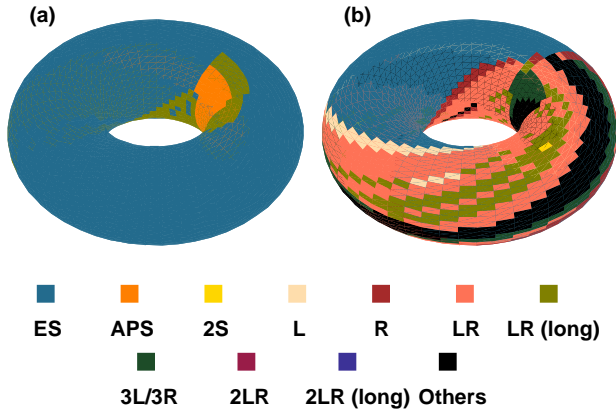


Fig. 4. Perturbation response ($\phi_i - \phi_p$) diagrams represented on a two-dimensional torus for a ring of $N = 20$ oscillators, initially in ES state, diffusively coupled to their nearest neighbors (via the inactivation variable). The nature of the ensuing defect patterns is indicated using the color scheme shown below the panels. The toroidal representation of the response diagrams arises naturally from the periodic nature of the phases ϕ_i and ϕ_p that correspond to the two axes of the toroid. The displayed figures, obtained for perturbation schemes (a) 1010... and (b) 101111..., represent the two topologically distinct classes of response diagrams that can be obtained for all the perturbation schemes that have been investigated. These correspond to the region in the ($\phi_i - \phi_p$) space where defects are generated forming either (a) an isolated patch or (b) a continuous ring that winds around the torus. Each oscillator is identical, being described by the parameter values $\epsilon = 0.001$, $k = 0.6$, $b = 0.1$ and $\alpha = 0.139$, and is coupled diffusively to each neighbour with strength $D_v = 1.13 \times 10^{-3}$.

unperturbed sites are indicated by 0. Thus, the perturbation pattern (or scheme) can be interpreted as a binary string corresponding to the input signal [Fig. 3 (a)]. The result of several different perturbation schemes, using perturbation response ($\phi_i - \phi_p$) diagrams, are shown in Fig. 3 (b-m). In these diagrams, the nature of the defect patterns obtained when a selected set of oscillators are perturbed from a specific initial phase ϕ_i to a given phase ϕ_p are shown. The precise pattern is determined using heuristically derived order parameters that utilize the qualitative differences between the panels of Fig. 2 (a), e.g., the total number of defects, the number of ‘‘long’’ defects, the direction in which the defects travel, etc. Specific sequence structures in the perturbation scheme are seen to yield predictable behavior in the response diagram. For example, a scheme involving an alternation of 0s and 1s, such as 1010... and 10101..., gives rise to large regions of APS in the phase response diagram. On the other hand, a scheme that has a contiguous sequence comprising an odd number of 1s, such as 1110... and 11111..., gives rise to large regions of LR (long).

While the response diagrams for different schemes differ greatly in their detailed nature we observe that, for the schemes we have investigated, the diagrams can be broadly classified into two topologically distinct categories. This is shown in Fig. 4, where the ($\phi_i - \phi_p$) space is projected onto a torus, a representation that arises naturally because of the periodicity of the phase angles ϕ_i and ϕ_p . In the first category, the region where defects are generated by the perturbation scheme is an isolated patch, while in the second, this region winds around the torus to form a continuous ring. This can be alternatively interpreted as follows: for one class of perturbation schemes,

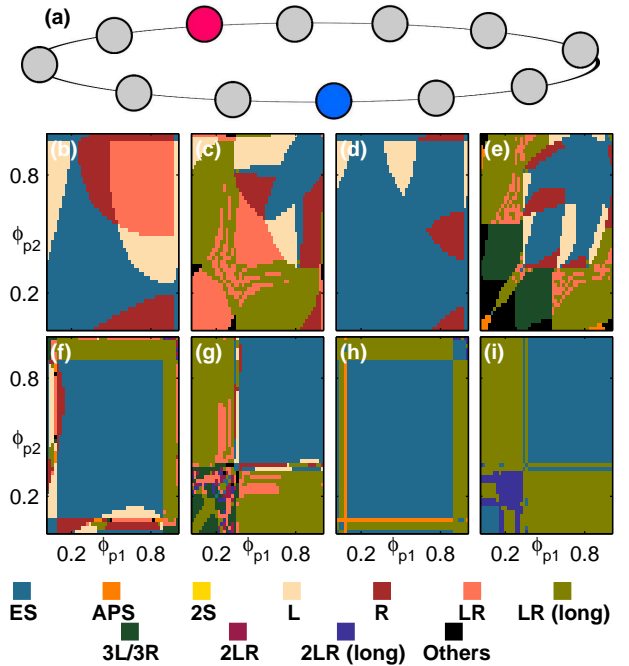


Fig. 5. (a) Schematic diagram illustrating the principle used to generate different types of defects by perturbing any two sites in a ring of exactly synchronized oscillators coupled diffusively to their nearest neighbors (via the inactivation variable). When the synchronized oscillators are at some phase ϕ_i on the limit cycle, different perturbations are applied to each of the two oscillators (shown in pink and blue) by changing their phases to ϕ_{p1} and ϕ_{p2} , respectively. As in Fig. 3 (a), the perturbation scheme illustrated in this schematic can have multiple representations because of the circular symmetry. One representation is $10^4 1 \dots$ (taking the bottom-most perturbed oscillator as the origin and moving clockwise), where 0 and 1 correspond to unperturbed and perturbed oscillators, respectively. (b-i) Perturbation response ($\phi_{p1} - \phi_{p2}$) diagrams indicating the nature of the defect patterns (represented using the color scheme shown below the panels) obtained when a system of $N = 20$ oscillators in an initial ES state is perturbed according to the principle outlined in (a). Each oscillator is identical, being described by the parameter values $\epsilon = 0.001$, $k = 0.6$, $b = 0.1$ and $\alpha = 0.139$, and is coupled diffusively to each neighbour with strength $D_v = 1.13 \times 10^{-3}$. The perturbation schemes used to generate the response diagrams shown in each panel for a specific initial phase ϕ_i are: (b) 11... at $\phi_i = 0.2$, (c) 11... at $\phi_i = 0.8$, (d) 101... at $\phi_i = 0.2$, (e) 101... at $\phi_i = 0.8$, (f) $10^3 1 \dots$ at $\phi_i = 0.4$, (g) $10^3 1 \dots$ at $\phi_i = 0.8$, (h) $10^9 1 \dots$ at $\phi_i = 0.4$ and (i) $10^9 1 \dots$ at $\phi_i = 0.8$. As in Fig. 3, $10^k 1$ indicates that there are k unperturbed oscillators between the two perturbed ones.

there exists a range of given initial phases for which it is not possible to perturb the system away from ES, while in the other class, for any initial phase ϕ_i , it is always possible to find a perturbed phase ϕ_p that will take the system away from ES. From our results it appears that when the perturbation scheme contains a subsequence ‘11’ (i.e., any two neighboring elements are perturbed) it belongs to the second class.

Using the above phenomenology, a possible principle for computation can be realized by applying perturbations to selected oscillators in the ring. In particular, we investigate the implementation of a two-input logic gate by perturbing a pair of elements that are initially in phase ϕ_i to phases ϕ_{p1} and ϕ_{p2} , respectively [Fig. 5 (a)]. Interpreting low and high values of ϕ_{p1} and ϕ_{p2} as 0 and 1, respectively, any combination of two binary inputs can be implemented. Fig. 5 (b-i) shows the result of several different perturbation schemes for given initial

phases ϕ_i , using perturbation response ($\phi_{p1} - \phi_{p2}$) diagrams. From this, we note that the perturbation either results in the system remaining in ES or transforming to a different state. If we consider the output to represent 1 when the perturbation results in a final state different from ES and 0 if not, we observe that certain schemes, such as $10^31\dots$ at $\phi_i = 0.8$, correspond to NAND logic. This is because only a high-high combination of ϕ_{p1} and ϕ_{p2} results in the system remaining in ES while the other combinations (viz., low-low, low-high and high-low) lead to defect states. As the NAND gate is considered to be a universal one, i.e., it can be used in combination to implement any other gate, this is a result of potential significance in using relaxation oscillator array dynamics for computation.

An alternative paradigm for implementing computation using the collective dynamics of coupled relaxation oscillators becomes apparent when we focus on the SPOD regime mentioned earlier. As oscillators are arrested in high or low values of the activation variable in this regime, a natural interpretation of the system state in terms of binary variables (viz., high=1, low=0) suggests itself. Thus, a perturbation that transforms a specific sequence of high and low values to another sequence can be interpreted as a computation that generates an output binary string from a given input string [Fig. 6 (a)]. In order to demonstrate this principle, we use a specific perturbation mechanism motivated by experiments involving light-sensitive oscillating chemical systems, where oscillations can be terminated by increasing the intensity of incident light [23]-[24]. We implement this in our model [Eqs. (1) and (2)] by introducing a parameter representing the intensity of the light stimulus inside the function $g(u, v)$, which governs the dynamics of the inactivation component v , similar to the formulation used in Ref. [25]. A perturbation of the same given magnitude is applied locally for a specific duration to a set of oscillators, which results in a reconfiguration of the initial SPOD state to a different one. An example is shown in Fig. 6 (b), where the perturbation can be interpreted as implementing a specific logic gate or a combination of gates in the neighborhood of the stimulated oscillators.

IV. CONCLUSION

To conclude, we have shown that a simple model of coupled relaxation oscillators that interact via diffusion of the inactivation component can give rise to a variety of spatiotemporal patterns that can be potentially useful for implementing computation. The generic nature of our model and its connection to previous experiments suggest that the ideas outlined here can be implemented using actual devices, for example, light-sensitive chemical systems [23]-[24]. Similarities between the relaxation oscillator system that we have used and a chain of trapped ions, as revealed by a recent theoretical study [26], suggest another system that could be used as an experimental test-bed for our results. Our exploratory study of the use of perturbations to (i) generate propagating configurations (involving phase defects) in a system of exactly synchronized oscillators, and (ii) transform one time-invariant pattern to another, suggests that these can be developed into schemes for implementing more complicated computations. Our demonstration of NAND logic in one of the implementations described above is of particular interest, as NAND gates are considered to be universal gates due to the fact that all

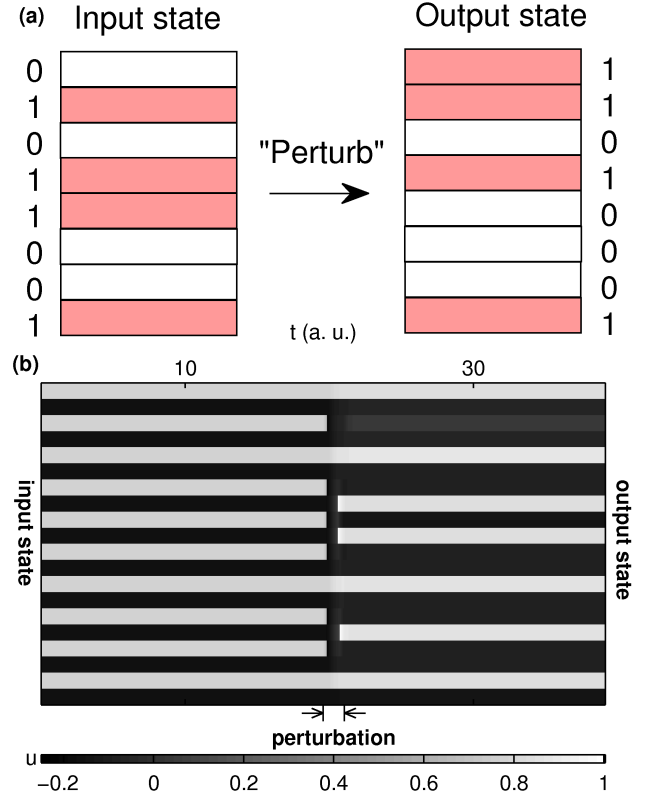


Fig. 6. (a) Schematic diagram illustrating a principle for computation that involves the transformation of system states in the SPOD regime via local perturbations, a specific example being shown in (b). The rows correspond to individual oscillators, with the colors representing whether the corresponding oscillator is arrested at a high (pink) or low (white) value of the activation variable. This sequence of high and low values can be read as a string of 1s and 0s, allowing us to map a particular state in the SPOD regime to a binary sequence. In this representation, the initial state of the system corresponds to an input binary string. Applying a local perturbation to specific oscillators results in a different configuration of high and low values that can be interpreted as the output binary string. Here, the activity following the perturbation represents the computation that transforms the input to the output. (b) The effect of local perturbations on the spatiotemporal evolution in a ring of $N = 20$ oscillators. The perturbation involves stimulating the inactivation component of six of the oscillators (corresponding to rows 3, 7, 9, 11, 15 and 17, counting from top) for a short duration as indicated in the figure. Subsequently, the system reorganizes into an altered SPOD state. Thus, the perturbation can be interpreted as a computation that transforms the input sequence $(10)^{10}$ to $10(001)^201(001)^30$. Note that in the local spatial neighborhood of an oscillator, the perturbation is functionally similar to a NOT logic gate. The individual oscillators in the figure are identical, being described by the parameter values $\epsilon = 0.001$, $k = 0.6$, $b = 0.1$ and $\alpha = 0.139$, and are coupled diffusively to their nearest neighbors through the inactivation variable with strength $D_v = 5 \times 10^{-3}$. Time is expressed in arbitrary units, normalized with respect to the period of the uncoupled oscillators.

possible logic gates can be constructed from combinations of NAND gates. We note that our work connects pattern formation in reaction-diffusion systems with the capacity for universal computation and provides an intriguing link between the two enduring legacies of Alan M. Turing [27]-[28].

ACKNOWLEDGMENT

The authors would like to thank Priyom Adhyapok for assistance in the initial stages of the project, Rajeev Singh, S. Sridhar and V. Sasidevan for helpful discussions and IMSC

for providing access to the supercomputing cluster “Satpura”, which is partially funded by DST. This research was supported in part by the IMSc Complex Systems Project.

REFERENCES

- [1] K. Zuse, “Calculating Space (*Rechner der Raum*),” Massachusetts Institute of Technology Technical Translation AZT-70-164-GEMIT, 1970.
- [2] J. A. Wheeler, “Information, physics, quantum: The search for links,” in *Proceedings of the 3rd International Symposium on the Foundations of Quantum Mechanics*, Tokyo, 1989, pp. 354-368.
- [3] R. P. Feynman, “Simulating physics with computers,” *Int. J. Theo. Phys.*, vol. 21, pp. 467-488, 1982.
- [4] W. H. Zurek, Ed., *Complexity, Entropy, and Physics of Information*. New York: Addison-Wesley, 1990.
- [5] J. P. Crutchfield, “Between order and chaos,” *Nature Physics*, vol. 8, pp. 17-24, 2012.
- [6] S. Sinha and B. K. Chakrabarti, “Dynamical transitions in network models of collective computation,” *Current Science*, vol. 77, pp. 420-428, 1999.
- [7] J. P. Crutchfield and M. Mitchell, “The evolution of emergent computation,” *Proc. Natl. Acad. Sci. USA*, vol. 92, pp. 10742-10746, 1995.
- [8] K. Lindgren and M. G. Nordahl, “Universal Computation in Simple One-Dimensional Cellular Automata,” *Complex Systems*, vol. 4, pp. 299-318, 1990.
- [9] S. Wolfram, “Statistical mechanics of cellular automata,” *Rev. Mod. Phys.*, vol. 55, pp. 601-644, 1983.
- [10] S. Sinha, “Phase transitions in the computational complexity of elementary cellular automata,” in *Unifying Themes in Complex Systems*, A. A. Minai and Y. Bar-Yam, Eds. Berlin: Springer, 2006, pp. 337-348.
- [11] M. Cook, “Universality in elementary cellular automata,” *Complex Systems*, vol. 15, pp. 1-40, 2004.
- [12] E. R. Berlekamp, J. H. Conway and R. K. Guy, *Winning Ways for Your Mathematical Plays*, Volume 2. New York: Academic Press, 1982.
- [13] R. Singh and S. Sinha, “Spatiotemporal order, disorder, and propagating defects in homogeneous system of relaxation oscillators,” *Phys. Rev. E*, vol. 87, 012907, 2013.
- [14] A. Hjelmfelt, E. D. Weinberger and J. Ross, “Chemical implementation of neural networks and Turing machines,” *Proc. Natl. Acad. Sci. USA*, vol. 88, pp. 10983-10987, 1991.
- [15] O. Steinbock, P. Kettunen and K. Showalter, “Chemical wave logic gates,” *J. Phys. Chem.*, vol. 100, pp. 18970-18975, 1996.
- [16] M. Prakash and N. Gershenfeld, “Microfluidic bubble logic,” *Science*, vol. 315, pp. 832-835, 2007.
- [17] A. Goldbeter, *Biochemical Oscillations and Cellular Rhythms*. Cambridge: Cambridge University Press, 1997.
- [18] B. C. Goodwin, “A statistical mechanics of temporal organization in cells,” *Symp. Soc. Exptl. Biol.*, vol. 18, pp. 301-326, 1964.
- [19] I. R. Epstein, “Can droplets and bubbles think?,” *Science*, vol. 315, pp. 775-776, 2007.
- [20] L. Blum, M. Shub and S. Smale, “On a theory of computation and complexity over the real numbers: NP-completeness, recursive functions and universal machines,” *Bull. AMS*, vol. 21, pp. 1-46, 1989.
- [21] J. D. Murray, *Mathematical Biology*, Volume 1. Berlin: Springer-Verlag, 2002.
- [22] M. Toiya, V. K. Vanag and I. R. Epstein, “Diffusively coupled chemical oscillators in a microfluidic assembly,” *Angew. Chem.*, vol. 47, pp. 7753-7755, 2008.
- [23] V. A. Vavilin, A. M. Zhabotinsky and A. N. Zaikin, “Effect of ultraviolet radiation on the self-oscillatory oxidation of malonic acid derivatives,” *J. Phys. Chem. (Moscow)*, vol. 42, pp. 3091-3094, 1968.
- [24] V. Gáspár, G. Basza and M. T. Beck, “The influence of visible-light on the Belousov-Zhabotinskii oscillating reactions applying different catalysts,” *Z. Phys. Chem. (Leipzig)*, vol. 264, pp. 43-48, 1983.
- [25] H. J. Krug, L. Pohlmann and L. Kuhnert, “Analysis of the modified complete Oregonator accounting for oxygen sensitivity and photosensitivity of Belousov-Zhabotinskii systems,” *J. Phys. Chem.*, vol. 94, pp. 4862-4866, 1990.
- [26] T. E. Lee and M. C. Cross, “Pattern formation with trapped ions,” *Phys. Rev. Lett.*, vol. 106, 143001, 2011.
- [27] A. M. Turing, “On computable numbers, with an application to the Entscheidungsproblem,” *Proc. Lond. Math. Soc.*, vol. 42, pp. 230-265, 1936.
- [28] A. M. Turing, “The chemical theory of morphogenesis,” *Phil. Trans. Roy. Soc. Lond. B*, vol. 237, pp. 37-72, 1952.